HEMODYNAMIC AND ELECTROPHYSIOLOGICAL EVIDENCE OF RESTING-STATE NETWORK ACTIVITY IN THE PRIMATE

296.11

A. Ardestani[1,2], W. Shen[1,2], F. Darvas[3], A. Toga[4], J.M. Fuster[1,2]

1. Semel Institute for Neuroscience and Human Behavior, UCLA, Los Angeles, CA, USA 2. Brain Research Institute, UCLA, Los Angeles, CA, USA 3. Dept. of Neurological Surgery, University of Washington, Seattle, WA, USA 4. Laboratory of Neuroimaging, Department of Neurology, UCLA, Los Angeles, CA, USA

INTRODUCTION

Most functional brain imaging studies rest on the premise that relative coactivations of the BOLD signal reflect coherent patterns of brain function. However, because the underlying hemodynamic trends are neither absolute nor direct measures of neural activity, analysis of BOLD signals alone may lead to inaccurate inferences about neural network organization. In light of this, much attention recently has been focused on understanding the patterns and mechanisms of intrinsic BOLD co-activations in the absence of any stimuli. Once regarded as physiological or methodological noise to be averaged out, the activity of so-called resting-state networks has been suggested to have an anatomical and functional basis. Numerous studies in the human and the monkey have shown electrophysiological and functional imaging evidence for spatially co-registered patterns of signal coherence. Still, the precise neural source of these coherent BOLD signals remains obscure. In this study we record four co-registered, complementary signal types – cortical oxygenation, surface field potentials (SFPs), local field potentials (LFPs), and multi-unit spiking activity (MUA) – to demonstrate coordinated cortical activity across a wide span of spatial localization and resolution. Of particular note is our use of near-infrared spectroscopy (NIRS) to measure oxygenation at a high temporal resolution (35ms) in a natural behavioral setting free of technical and anesthesia artifacts. Demonstration of hemodynamic and electrophysiological manifestations of "spontaneous" neural activity will help elucidate the properties of non-task related brain activations that can be utilized to improve BOLD signal interpretation. Furthermore, inasmuch as resting-state networks are modulated in active brain states, characterization of their behavior during resting conditions could provide important information for understanding normal and pathological brain functioning.

MATERIALS AND METHODS

Data were obtained from four male rhesus macaques trained to sit motionless in a quiet dark room. Eye movements were recorded using an ISCAN infrared tracking system to ensure the subjects' wakefulness, and body motion was monitored to restrict data collection to periods free of extraneous activations. Surgical implants allowed direct recording access to cortical regions that harbor well recognized frontal-posterior neural networks (Fig. 1). Eight channels of spatially overlapping NIRS signals and surface field potentials (SFPs) were acquired epidurally from both regions of interest through optodes and electrodes embedded in plastic probes (Fig. 2). Light from a halogen source was filtered between 650nm and 1000nm (Oriel Instruments) and directed onto the brain surface via the light emitting optode. Reflected light from the illuminated cortex was detected by the detecting cables and fed into eight spectrophotometers (S-2000 Spectrophotometer, Ocean Optics), dispersed over a wavelength range of 780nm to 910nm, scanned by a CCD array every 35ms, and submitted to a modified Beer-Lambert analysis to calculate fluctuations in oxy- (HbO_2) and deoxy-hemoglobin (HbR) concentration. At the same time, SFPs were recorded at 1kHz, amplified 1000x, and band-passed between 0.1-100Hz. Finite Element Modeling (FEM) of photon propagation and charge distribution through the cortex was applied to measure corresponding spatial sensitivities of each signal type (Fig. 3, FEM courtesy of Dr. Richard Leahy and Belma Dogdas, Signal and Image Processing Institute, USC). In alternating sessions, four simultaneously acquired channels (two per region) of LFP and MUA signals were also recorded. LFPs were obtained through low-pass filtering of the mean extracellular field potential and processed, as were the SFPs. Concomitant MUA records (not featured here) were derived from the same broadband neurophysiological signal and plotted as frequency histograms. Multiple microelectrode penetrations permitted LFP and MUA sampling that was spatially equivalent to that of the other recording techniques. Signals of all types were acquired during sequential epochs of 20s-length.
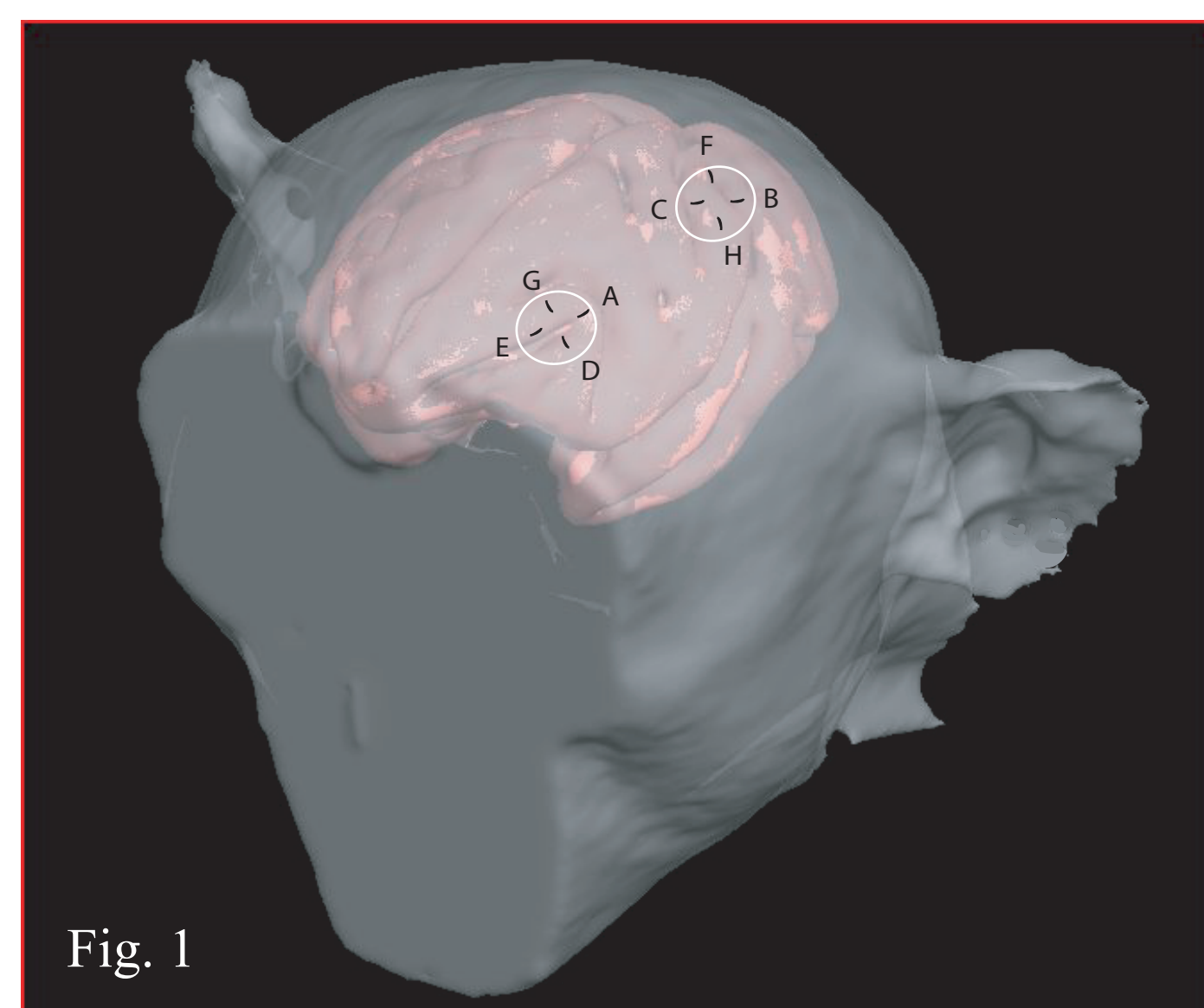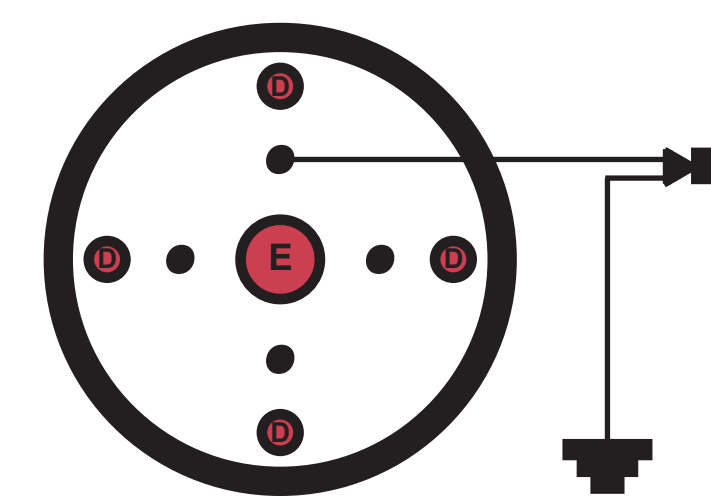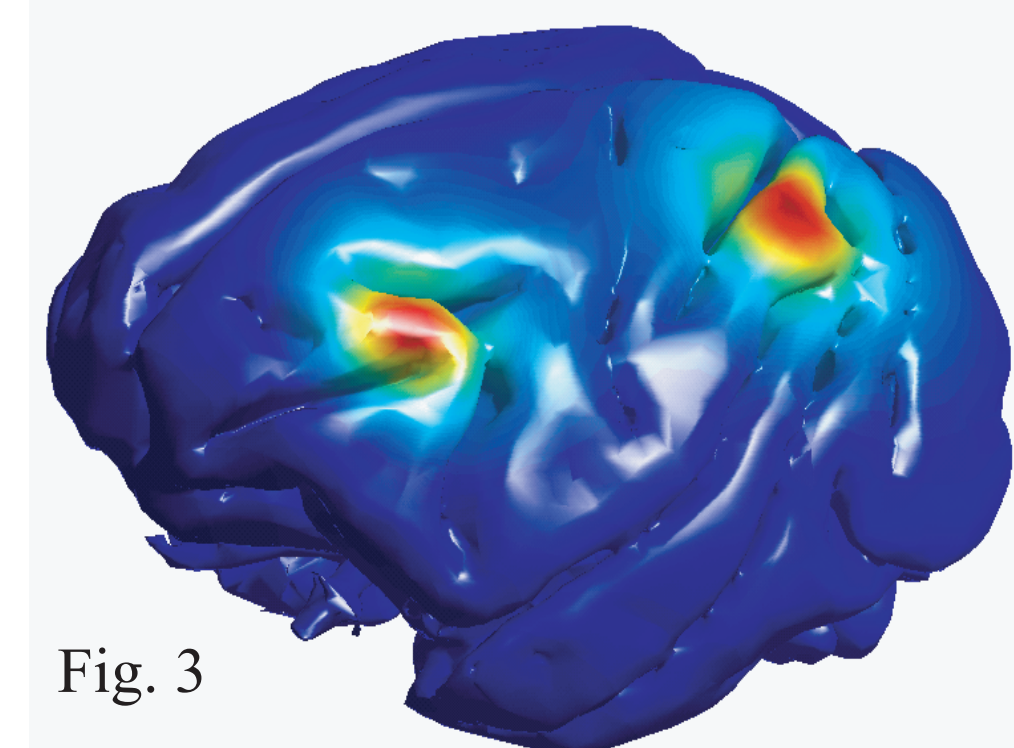

Fig. 1

Fig. 2

Fig. 3

ANALYSIS:

All acquired data were first screened for excessive movement and artifact. Next, the signals and cross-cortical interactions were quantified in the frequency and time domains. Specifically:

Near Infrared Spectroscopy: The power spectra and time-frequency plots of oxygenation trends in each channel were first calculated in order to identify characteristic slow (<0.1Hz) BOLD fluctuations that define resting-state networks. Hb02 trends were submitted to a covariance analysis to visualize signal coactivations between prefrontal and posterior parietal regions. A 2.6s sliding window was used to calculate the time-varying correlation between individual epochs, assuming zero lag between signals from the two regions, for all pairs of channels.

Surface Field Potentials: Power spectra and time-frequency plots for each channel were calculated to detect synchronization in discrete frequency bands. Raw voltage curves were filtered into five frequency bands (1-4Hz, 5-8Hz, 9-14Hz, 17-23Hz, and 75-90Hz), and the average power in each band plotted over time (band-limited power, BLP). Interactions between pairs of channels were illustrated in coherence plots from 1Hz to 100Hz.

Local Field Potentials: The frequency profiles and spatial interactions of LFPs were analyzed using the same methods as for SFPs.
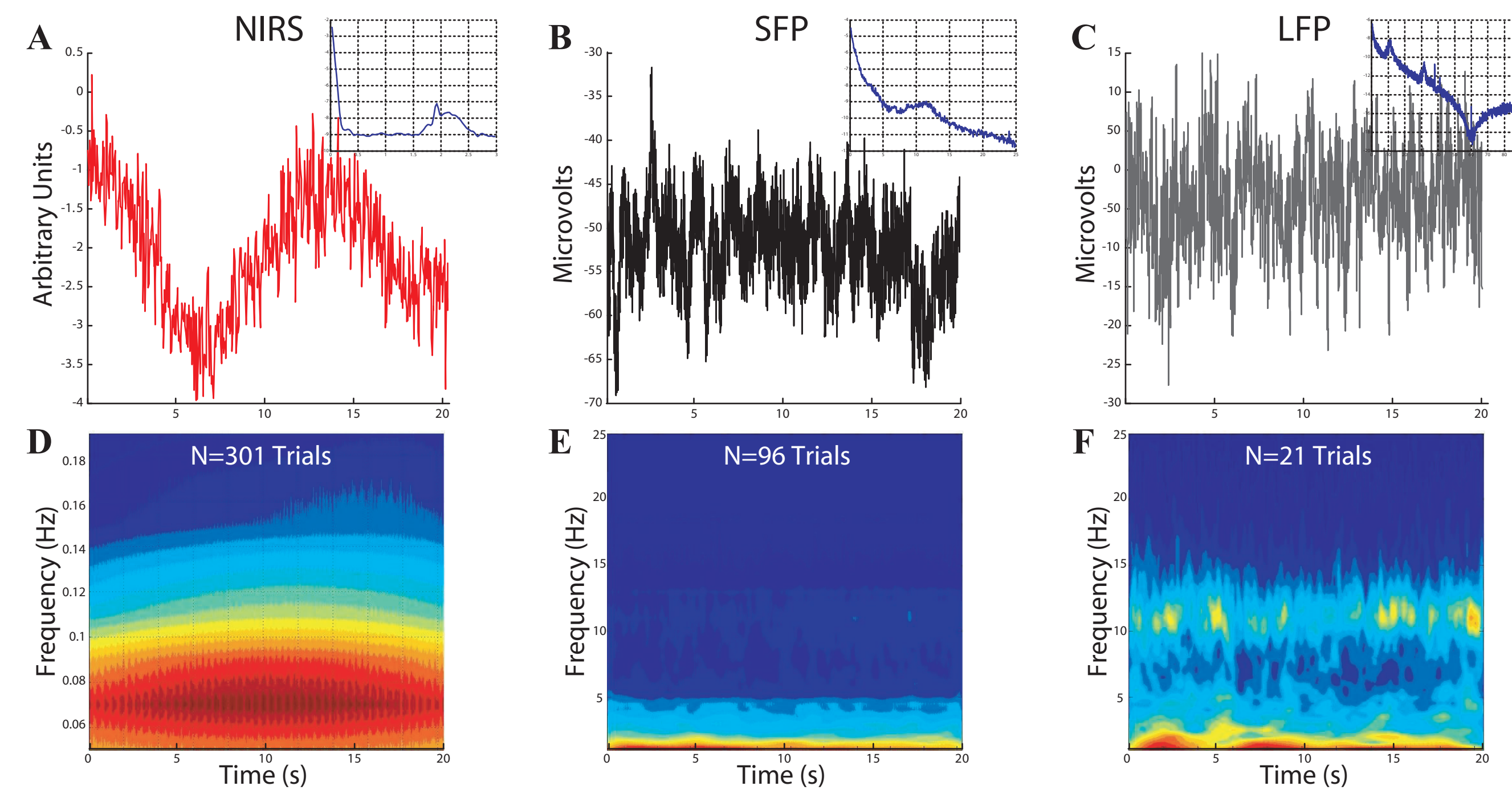
RESULTS

Fig. 4. Representative data samples. Graphs A-C illustrate three signal types recorded from dorsolateral prefrontal cortex (DPC) in a single monkey. Graph A shows an HbO_2 profile with a cycle period of approximately 12.5s. The inset power spectrum shows a strong low frequency (<0.1Hz) component, as well as peaks related to cardiac (~2.1Hz) and respiratory (~0.3Hz) oscillations. Graph B depicts an SFP curve, and C an LFP trace recorded 2.64mm into the cortex. The inlaid power spectra exhibit characteristic 1/f decay in overall power and pronounced peaks at the alpha and beta frequency ranges. A notch filter centered at 60Hz produced the midrange decrease in power. In graphs D-F, time-frequency plots calculated for multiple sessions reveal synchronization trends for each signal type. The HbO_2 signal power in D shows an increase in the 0.06-0.08Hz range, while both types of field potentials (E-F) exhibit synchronized oscillations in several frequency bands.
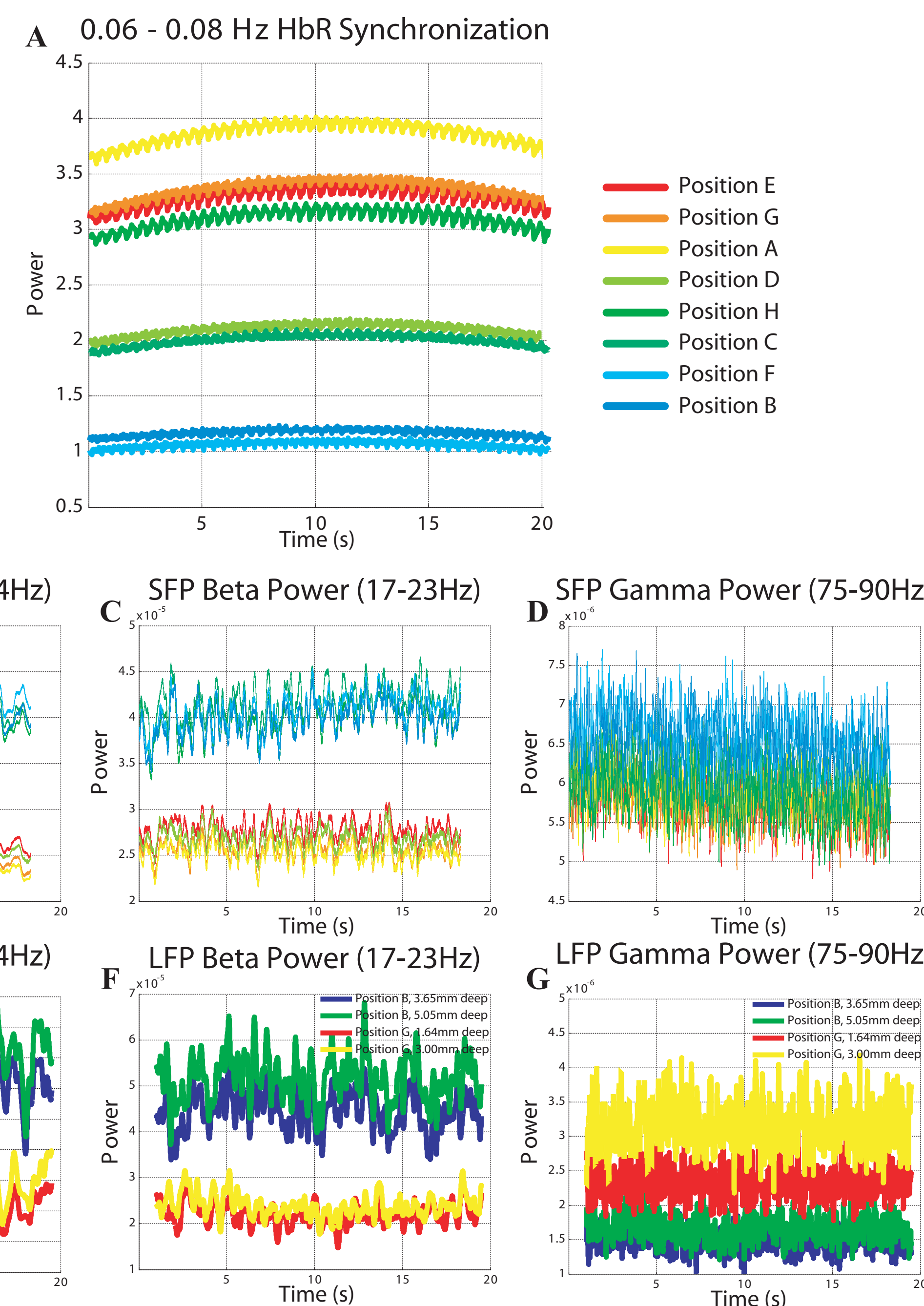

Fig. 5. NIRS and SFP signal properties across a frontal-parietal network. In graph A, a plot of average power in the 0.06-0.08Hz range reveals marked variability in the frequency properties of the HbR signal across all eight channels. Generally, the prefrontal channels in all monkeys show stronger signal synchronization than do parietal channels. A spatially analogous signal pattern is seen in SFP and LFP power trends. Graphs B-G show power trends in the alpha, beta, and gamma ranges for both SFP and LFP records from corresponding cortical positions. In all monkeys and frequency bands, signals cluster with respect to cortical area (i.e., frontal or parietal), with parietal cortex exhibiting greater synchronization than prefrontal cortex. Interregional differences in BLP are less pronounced in the gamma range than in other frequency bands. Notably, neural synchronization in most bands tends to correlate inversely with the hemodynamic synchronization apparent in the corresponding HbR curves above (A).
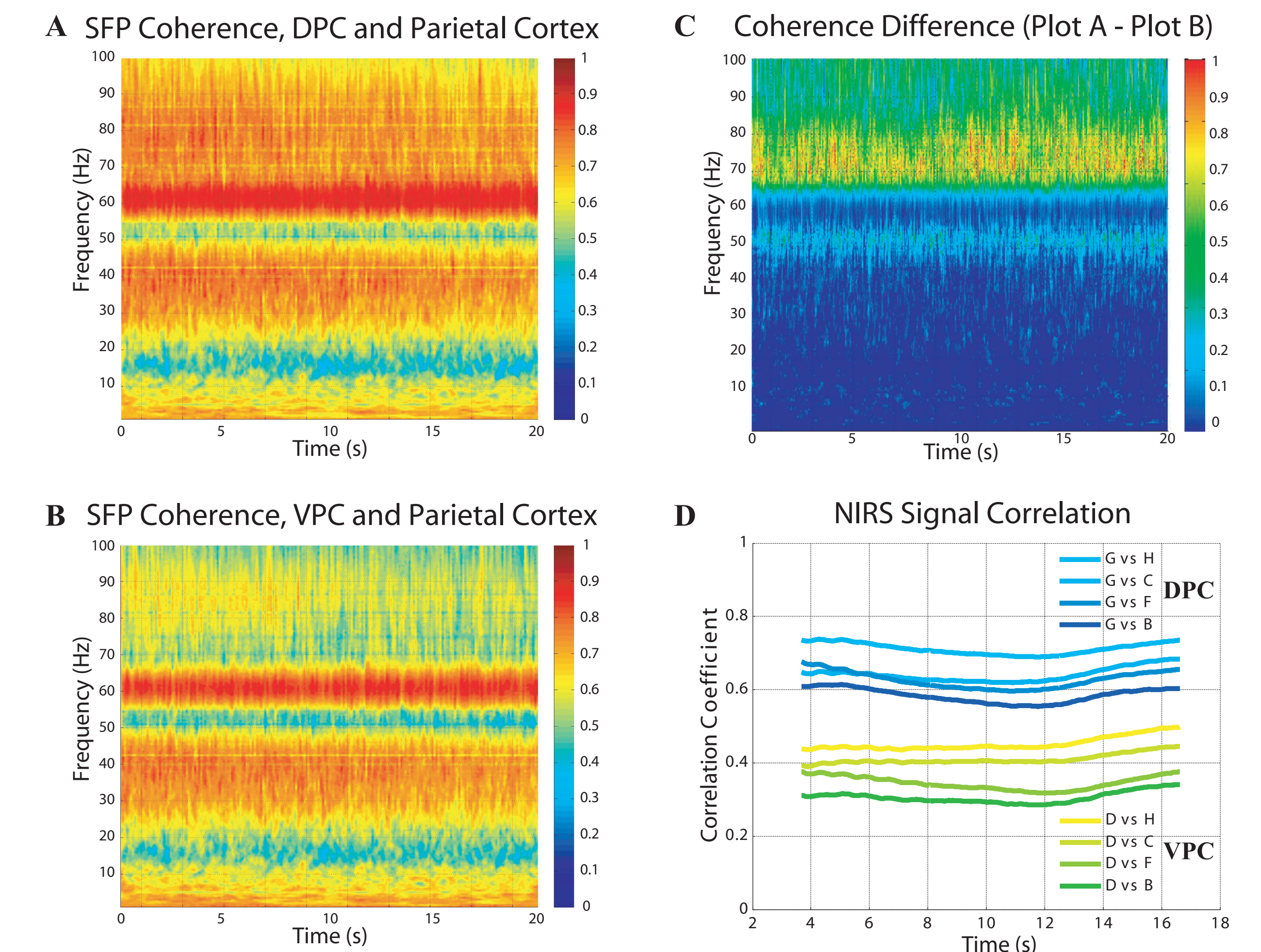

Fig.6. Signal coactivations between regions. Coherence plots for both DPC-parietal (Graph A) and VPC-parietal (Graph B) SFP pairs show marked SFP coherence in the delta, gamma, and high-gamma ranges (a strong band appears at 60Hz due to power line artifact). Subtraction of the two coherence plots shows that the relative increase in DPC-parietal coherence is reflected primarily in the 45-55Hz and the 65-85Hz ranges (Graph C). An analogous pattern of spatial differentiation is seen in NIRS signal covariance within the same regions. Graph D depicts correlation values between DPC-parietal and VPC-parietal HbO_2 channel pairs in one monkey (N=302 epochs). In all monkeys, parietal NIRS activations correlate better with those of DPC than with those of VPC.

DISCUSSION

The present data demonstrate spatially corresponding patterns of hemodynamic and electrophysiological coactivations that are consistent with those reported in the human literature. Our findings are unique, however, in that they reveal intrinsic network activations in the unanesthetized monkey. Additionally, the fast sampling rate afforded by NIRS disambiguates the cardiac and respiration pulses that can alias as slower oscillations when using fMRI BOLD imaging.

The spatial patterning of signal power suggests that both electrophysiological and vascular fluctuations are modulated in the frequency domain in a functionally relevant manner. The BLP of surface and local field potentials in the alpha and beta frequency bands appear systematically clustered by cortical region. Likewise, signal power of slow (<0.1Hz) oscillations of HbR concentration – physiologically coupled inversely to the BOLD signal – also generally segregate with respect to cortical location. Both patterns are in contrast with the relatively invariant gamma-band BLP cortical distribution. Gamma-band FP oscillations are widely implicated in the functional connectivity linking anatomically distant nodes of neural networks. The resilience of the gamma-band interregional coherence is consistent with the results of a previous study (Leopold et al., 2003). Ultimately, temporal trend analysis would be best to evaluate the time-varying relationship between FP power and hemodynamic signal magnitudes and oscillations.

The present observations of signal coactivations in the resting state are consistent with anatomical and physiological differences described within prefrontal cortex in cognition. Differences in both gamma-band coherence and in NIRS signal covariance between DPC-parietal and VPC-parietal channel pairs (Fig. 6) suggest a tighter functional coupling of parietal cortex with dorsal prefrontal, rather than with ventral prefrontal subregions. This suggests that the interaction between hemodynamic and electrophysiological fluctuations may indeed form the neurovascular basis for functional network engagement in resting and active cortical states.

CONCLUSION

Coordinated BOLD fluctuations that are observed in the absence of external stimuli are rooted in neural activity, especially in the gamma band, and not simply an expression of passive vascular phenomena.

REFERENCES

Fox MD, Raichle ME. Spontaneous fluctuations in brain activity observed with functional magnetic resonance imaging. Nat Rev Neurosci. 2007 Sep;8(9):700-11.

Leopold DA, Murayama Y, Logothetis NK. Very slow activity fluctuations in monkey visual cortex: implications for functional brain imaging. Cereb Cortex. 2003 Apr;13(4):422-33.

Mantini D, Perrucci MG, Del Gratta C, Romani GL, Corbetta M. Electrophysiological signatures of resting state networks in the human brain. Proc Natl Acad Sci U S A. 2007 Aug 7;104(32):13170-5.

Shmuel A, Leopold DA. Neuronal correlates of spontaneous fluctuations in fMRI signals in monkey visual cortex: Implications for functional connectivity at rest. Hum Brain Mapp. 2008 Jul;29(7):751-61.